IEEE Access
Multidisciplinary | Rapid Review | Open Access Journal

Received June 3, 2019, accepted July 5, 2019, date of publication July 10, 2019, date of current version July 29, 2019.

Digital Object Identifier 10.1109/ACCESS.2019.2927680

A New Technology Applied to Power System Stability Control: Phase Sequence Exchange Technology

SHAOFENG HUANG[1,2], (Member, IEEE), YIFAN LI[1], HUI LI[1], AND YILING HUANG[1]
[1]State Key Laboratory of Alternate Electrical Power System with Renewable Energy Source, North China Electric Power University, Beijing 102206, China
[2]Beijing Sifang Automation Company Ltd., Beijing 100085, China

Corresponding author: Yifan Li (ivanlee_lyf@163.com)

This work was supported in part by the Beijing Sifang Automation Company Ltd., under Grant KH17010347, and in part by the Fundamental Research Funds for the Central Universities under Grant JB2019180.

ABSTRACT AC transmission systems are often affected by stability issues. During the design phase of such systems, their ability to cope with the various kinds of disturbance is taken into consideration, however, sudden large disturbances may still result in power angle instability, which can greatly increase the risk of an overarching power system break down. Therefore, the development of a safety protection system is a priority in the field of power system construction. In response to this problem, we propose a new exploratory solution strategy – Phase Sequence Exchange Technology (PSET). The PSET can be summarized as follows: when the power angle of an equivalent dual power supply system swings to a suitable angle between 90° and 180°, disconnect the primary side phase of the communication line by power electronic equipment and causing the swift misalignment of the connection. The A, B, C three-phase sequence then, connects to the three-phase C, A, B sequence. The PSET instantaneously realizes this change and reduces the power angle by 120°, pulling the formerly increasing power angle back to a smaller angle and preventing the system from becoming imbalanced. In this paper, the mechanism which improves the stability of the PSET is explained by using the equal area rule. The threshold of the PSET work angle is determined by the energy function and the unbalanced potential energy in the system that can be effectively reduced by the PSET. Based on these findings, the phase trajectory method is used to determine the evaluation criteria for the PSET. This allows us to establish whether the PSET is effective by examining the state of the system after the fault is removed. Finally, an example is given in order to verify the effectiveness of the PSET and to prove that PSET is able to prevent the system from becoming imbalanced while still maintaining its structural integrity.

INDEX TERMS Transient stability emergency control, phase sequence exchange technology, power electronic equipment, effective criterion.

I. INTRODUCTION

Instability is the most significant problem affecting AC transmission systems [1]. The current expansion of the power grid and the simultaneous increase in regional interconnections has led to a range of unpredictable operating variables and complex disturbance factors within the system. These variables can influence each other, ultimately causing a power swing of the tie line and significantly increasing the transient instability of the system. These swings pose a significant threat to the safe and stable operation of the system [2]–[6].

The generator is the most fundamental component of any power system. After a large disturbance, the rotors of each generator oscillate relative to one another, causing the power angle to change constantly. Analyzing the trend of power angle variation in this scenario constitutes the bulk of current transient stability research [7]. Generally, if the rotor is always bounded relative to the rocking angle, the system is synchronously stable; conversely, if the relative angle between the rotors eventually increases, the system will lose synchronization stability [8]–[12]. In terms of transient power angle instability, the issue of how to implement control measures that will help restore system restore stability remains an urgent and unresolved issue.

The associate editor coordinating the review of this manuscript and approving it for publication was Tariq Masood.

Relevant potential solutions to the transient stability problem can be divided into two categories: firstly, primary system means and, secondly, the secondary system means [13]. The primary system means generally consist of increasing grid structure and adding series capacitor compensation in order to reduce the electrical distance between the sending end and the receiving end. This can be achieved by using a DC power transmission scheme, and installing a static reactive power compensation device in order to support the voltage [14], [15]. However, these measures often need to be completed in the initial stages of power grid planning and construction, and are frequently limited by funds, policy, geography and other factors [16]–[21]. Secondary system means usually involve increasing a system's damping. This method provides damping torque in order to suppress transient instability and also includes the addition of a control device, which improves system stability [22], [23]. The secondary system approach has significant advantages in terms of ease of implementation and economy, so these methods have become essential in the project of reducing regional transient instability [24], [25]. The secondary means can be further divided into two categories – power supply side measures and grid side measures. The power supply side measures are controlled by generators, including power system stabilizers (PSS) and generator mechanical power input modulation, such as fast-closing valves [24], [26]. The controlling factors of the grid side measures consist of equipment within the network, including the transformer's neutral point via low resistance grounding, the FACTS component, high voltage direct current transmission and the energy storage system (Energy Storage Devices) [27], [28].

During the Conference International des Grands Reseaux Electrique, it was concluded that implementing these measures would also include cutting, load shedding, low frequency load shedding, and out-of-step disengagement. The common goal of these measures is to help restore a system's stability via emergency controls that disrupt the integrity of the grid [29]. Restoring the stable operation of the system by destroying the integrity of the power grid is a measure that should only be taken as a last resort [30]. A superior option would be a control measure that can not only maintain the integrity of the power grid structure, but also calm the oscillation of the system. In view of this objective, we propose a new stable control measure - ''phase sequence exchange technology'' or PSET.

PSET can be summarized as follows: when the power angle of the equivalent dual power supply system swings to a suitable angle between 90° and 180°, disconnect the primary side phase of the communication line by power electronic equipment, causing the swift misalignment of the connection. The A, B, C three-phase sequence then connects to the three-phase C, A, B sequence. The PSET realizes the instantaneous change and reduces the power angle by 120°, pulling the initially expanding power angle back to a reduced state, thereby restraining the system from falling out-of-step. Based on the equal-area criterion, PSET reduces the power angle and increases the generator's output of electromagnetic power, thereby expanding the deceleration area and improving the overall stability of the system.

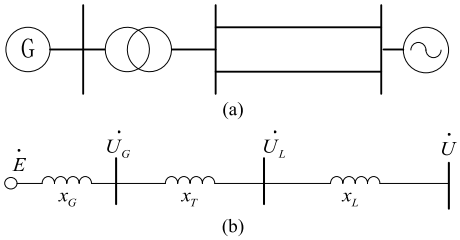

FIGURE 1. OMIB system diagram and equivalent circuit diagram.

The main objectives of this paper are as follows:

1. We propose a new stability control measure, which can restrain the system from falling out-of-step while maintaining the structural integrity of the power grid;
2. We explain the mechanism of the PSET used to improve the stability of the system and determine the behavioral criteria of the PSET;
3. We establish a criterion for judging whether the PSET can be effective;
4. We provide an example to verify the effectiveness of the PSET, and to prove that it is able to restrain the system from experiencing an out-of-step condition while still maintaining the overall structural integrity of the system.

The chapters of this paper are arranged as follows: Section II introduces the basic principles of the commutation sequence technique, and uses the equal area rule and the transient energy function to explain the mechanism used for improving the system's stability via phase sequence exchange technology; in Section III, the criteria of the PSET is validated; Section IV verifies the effectiveness of the commutation sequence technique by actual system simulation; our concluding remarks are provided in Section V.

II. THE BASIC PRINCIPLES OF PHASE SEQUENCE EXCHANGE TECHNOLOGY

A. MODEL

In this section, the influence of phase sequence exchange on the stability of a one-machine to infinite bus (OMIB) system is analyzed on the basis of the equal area criterion and the transient energy function.

The OMIB system is shown in Fig. 1:

A major feature in traditional methods of analysis is the simplified, or classical, model of the generator. Here, the machine is modelled by an equivalent voltage source behind an impedance. The assumptions behind the model are as follows:

1. Voltage regulators are not present and manual excitation is used. This implies that in a steady-state, the magnitude of the voltage source is determined by the field current, which is constant.
2. Flux decay in the field circuit is neglected (This is valid for a very short period, say one second, following a

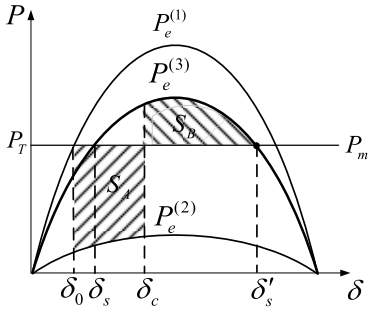

FIGURE 2. Equal-area criterion.

disturbance, as the field time constant is of the order of several seconds).

3. The mechanical power input to the generator is constant [31].

In this work, the dynamics of OMIB are modeled by the swing equation

$$\begin{cases} \dot{\delta} = \omega \\ M\dot{\omega} = -P_e \sin\delta + P_m - D\omega \end{cases} \tag{1}$$

where the rotor angle δ represents the angle by which $\dot{E}$ leads $\dot{U}$. M is the inertia constant, P_m is the mechanical power input, P_e is the electrical power output, D is the damping coefficient, and ω is the speed deviation.

The reactance between $\dot{E}$ and the infinite system is:

$$x_\Sigma = x_d' + x_T + x_L \tag{2}$$

The generator's electrical power P_e is:

$$P_e = \frac{E'U}{x_\Sigma}\sin\delta \tag{3}$$

As seen in Fig. 2, the steady-state power angle is $\delta = \delta_0$ and the electrical power is $P_e^{(1)}$.When $t = t_0$, a three-phase fault occurred on one of the lines, and the electrical power changed to $P_e^{(2)}$. In this stage, the generator accelerates and the power angle δ increases until the fault line is removed and the electromagnetic power changes to $P_e^{(3)}$.

In Fig. 2, δ_s is the stable equilibrium point after the removal of the fault, and δ_s' is the unstable equilibrium point.

The acceleration area is:

$$S_A = \int_{\delta_0}^{\delta_c} \left(P_m - P_e^{(2)}\right) d\delta$$

And the deceleration area is:

$$S_B = \int_{\delta_c}^{\delta_s'} (P_e^{(3)} - P_m) d\delta$$

If $S_A > S_B$, the system will experience a loss of synchronism [32].

B. FUNDAMENTALS OF PHASE SEQUENCE EXCHANGE TECHNOLOGY

With regards to the above-mentioned generator acceleration and instability scenario, when the system is out-of-step and the power angle has swung to a certain angle between 90°-180°, the phase sequence exchanging operation can be used to restrain the system from entering an out-of-step condition. The power angle threshold of the PSET is set to δ_m. When the system is out-of-step and the power angle swings to δ_m, using power electronic equipment quickly misaligns the connection by disconnecting the primary side phase of the contact line. The A, B, C three-phase sequence then connects to the three-phase C, A, B sequence, instantaneously reducing the angle by 120° and thus restraining system from entering an out-of-step condition. The power angle vector diagram is shown in Fig. 3:

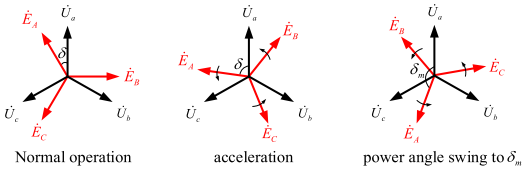

FIGURE 3. Three-phase power angle vector diagram.

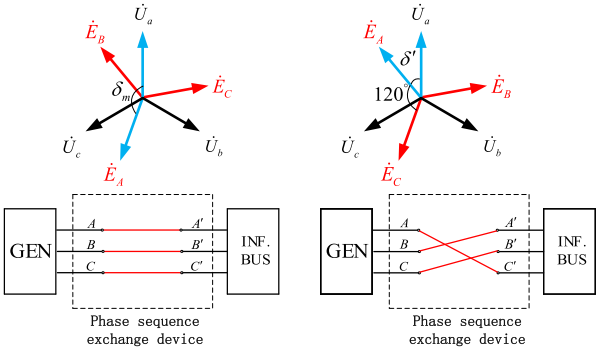

FIGURE 4. Vector diagram and phase sequence connection diagram of phase A.

We now examine the phase sequence exchange when $\delta = \delta_m$. Take phase A, where the power angle, δ_A, before the phase sequence exchange is the angle between phasor $\dot{E}_A$ and $\dot{U}_a$. After the phase sequence exchange, the power angle δ_A is the angle between the phasor $\dot{E}_B$ (changed to $\dot{E}_A$ after the phase sequence exchange) and $\dot{U}_a$. The vector diagram of phase A and the phase sequence connection diagram are shown in Fig. 4, where it can be seen that the phase sequence exchange reduces the power angle of the system by 120°:

C. THE POWER ANGLE THRESHOLD OF PHASE SEQUENCE EXCHANGE TECHNOLOGY

For the swing equation (1), the unbalanced kinetic energy of the system after the fault line resection can be expressed as.

$$V_k = \frac{1}{2}M\omega^2 \tag{4}$$

Unbalanced potential energy of the system.

$$V_p = \int_{\delta_s}^{\delta} (P_e^{(3)} - P_m) d\delta = P_e(\cos\delta_s - \cos\delta) + P_m(\delta_s - \delta) \tag{5}$$

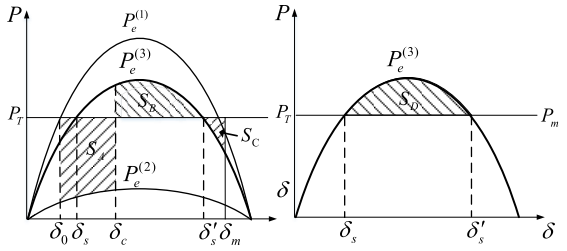

FIGURE 5. Power-angle curve before and after the phase sequence exchange.

The phase sequence exchange reduces the power angle of the system by 120°, but does not directly change the speed of the generator. Therefore, the PSET only changes the potential energy of the system but does not change the kinetic energy of the system. If δ_s is selected as a potential reference point, there is $V_p|_{\delta=\delta_s} = 0$ [33]. Therefore, if the power angle threshold of the PSET is set to $\delta_m = \delta + 120°$, the power angle of the system after the phase sequence exchange is changed to δ_s once more, which has the ability to eliminate all the unbalanced potential energy in the system.

In Fig. 5, the phase sequence is exchanged at the power angle $\delta_m = \delta + 120°$, so that the work angle decreases from 120° instantly and the system's work angle becomes δ_s. The electrical power output increases instantaneously, and the system re-enters the entire deceleration area, S_D, thus increasing the stability of the system.

Therefore, the power angle threshold of PSET is set to $\delta_m = \delta + 120°$.

III. EFFECTIVE CRITERION OF PHASE SEQUENCE EXCHANGE TECHNOLOGY

A. EFFECTIVE CONDITION

Here we examine the analysis in the previous section. In Fig. 5, the phase sequence is exchanged at the power angle of $\delta_m = \delta + 120°$, and the system re-enters the entire deceleration area, S_D, thus increasing the stability of the system. In this scenario there are three potential situations:

Firstly, if $S_B + S_D \geq S_A + S_C$ then the deceleration area of the system is greater than the acceleration area after the phase sequence exchange, and the system can resume synchronization.

Secondly, if $S_B + S_D < S_A + S_C$ but $S_D > S_C$, the deceleration area of the system is still less than the acceleration area after the phase sequence exchange. However, the phase sequence exchange causes the system to enter the deceleration area again larger than the acceleration area. Therefore, after several phase sequence exchanges, the deceleration area of the system will eventually be greater than the acceleration area, and the system can resume synchronization.

Thirdly, if $S_D < S_C$, the phase sequence exchange makes the deceleration area smaller than the acceleration area, meaning that the phase sequence exchange is not conducive to stabilizing of the system. In this case, the commutation sequence operation has no effect.

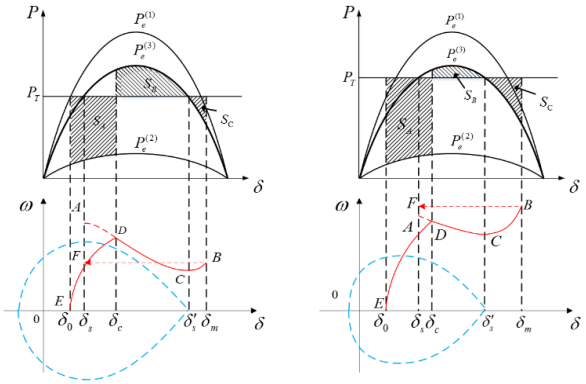

FIGURE 6. EAC and phase trajectory diagram.

In this section, the effect of system damping is further considered, and we use the phase trajectory diagram and the rotor swing equation to calculate effective conditions for the commutation sequence.

In Fig. 6, the blue dotted line demarcates the stability domain of the system, and the red solid line is the fault trajectory and rotor trajectory of the system. The E-D segment corresponds to the system experiencing the acceleration area S_A, the fault is cut off at point D, the D-C segment corresponds to the deceleration area S_B, the power angle at point C is δ'_s, the C-B segment corresponds to the acceleration area S_C, the B point power angle is $\delta_s + 120°$, and the F phase is reached after the phase sequence exchange. If point F is in the stable domain of the system, the system can be pulled back to synchronization.

Point A is obtained by extending the rotor trajectory to δ_s after the removal of the fault.

If the power angle of the system returns to δ_s after the phase sequence exchange, and if the speed is lower than the speed before the phase sequence exchange, as shown in Fig. 6 (a), the phase sequence exchange will reduce the speed deviation of the system, meaning that the phase sequence exchange is effectively improving the stability of the system.

If the power angle of the system returns to δ_s after the phase sequence exchange, and if the speed is greater than the speed prior to the phase sequence exchange, as shown in Fig. 6 (b), the phase sequence exchange is increasing the speed deviation of the system and therefore is not improving the stability of the system.

That is to say, the effective conditions for the use of PSET is $\omega_A > \omega_B$.

B. EFFECTIVE CRITERION

When $\omega_A > \omega_B$ on the same rotor trajectory, the phase sequence exchange is effectively able to improve the stability of the system. For the swing equation:

$$M\frac{d^2\delta}{dt^2} + D\frac{d\delta}{dt} = P_M - P_E \sin\delta$$
$$\omega_A = \left.\frac{d\delta}{dt}\right|_{\delta=\delta_S}, \omega_B = \left.\frac{d\delta}{dt}\right|_{\delta=\delta_m},$$
$$\text{where } \delta_m = \delta_s + 120°. \quad (6)$$

TABLE 1. Fitting I.

	Standard error	standard coefficient	t	Sig
P_e	0.075	-0.002	-0.0151	0.880
P_m / P_e	0.149	-0.887	-78.670	0.000
D	0.040	0.522	65.998	0.000
M	0.047	-0.095	-12.174	0.000

TABLE 2. Fitting II.

	Standard error	standard coefficient	t	Sig
P_m	0.097	-0.011	-1.103	0.270
P_m / P_e	0.132	-0.879	-87.953	0.000
D	0.040	0.523	66.031	0.000
M	0.047	-0.095	-12.170	0.000

The equation has a unique solution so long as the system parameters are determined and the initial values are given [34].

Substituting $\delta = \delta_S$ and $\delta = \delta_m$ into the rotor sway equation, means that ω_A, ω_B can be obtained numerically. When the system parameters (M, D, P_M, P_E) change, the solution of ω_A, ω_B will also change. For any set of M, D, P_M, P_E, there is only one set of ω_A, ω_B that corresponds. Suppose their correspondence is as follows.

$$\omega_A = f_1(M, D, P_M, P_E) \tag{7}$$
$$\omega_B = f_2(M, D, P_M, P_E) \tag{8}$$

The system loses synchronization when the power angle reaches δ_B, therefore $\omega_B \neq 0$.

Divide (7) by (8).

$$\frac{\omega_A}{\omega_B} = \frac{f_1(M, D, P_M, P_E)}{f_2(M, D, P_M, P_E)} = f(M, D, P_M, P_E) \tag{9}$$

That is, the effective conditions for the PSET is $\frac{\omega_A}{\omega_B} > 1$.

$$f(M, D, P_M, P_E) > 1 \tag{10}$$

Consider the actual situation of the system operation, we set $M \in [6, 8]$, $D \in [0, 2]$, $P_e \in [1.8, 2.1]$, $P_m \in [1.4, 1.6]$, and the unit is the standard value. Within this range, two thousand sets of data are randomly generated using the Monte Carlo method, and ω_A, ω_B corresponding to each set of data is obtained by using the improved Euler method. The obtained data is a 2000×6 matrix as follows:

$$A = \begin{bmatrix} M_1 & D_1 & P_{m1} & P_{e1} & \omega_{A1} & \omega_{B1} \\ M_2 & D_2 & P_{m2} & P_{e2} & \omega_{A2} & \omega_{B2} \\ \vdots & & & & & \\ M_n & D_n & P_{mn} & P_{en} & \omega_{An} & \omega_{Bn} \end{bmatrix} \tag{11}$$

To obtain the analytical expression of equation (10), regression analysis is required for M, D, P_M and P_E. The results of regression analysis for $M, D, P_M, P_M/P_E$ and $M, D, P_M/P_E$, P_M are as follows.

In the table, t is the significant test value, Sig is the significance, and ω_A/ω_B is the dependent variable. When the absolute value of the standard coefficient of the independent variable is less than 0.3, its influence on the dependent variable can be ignored.

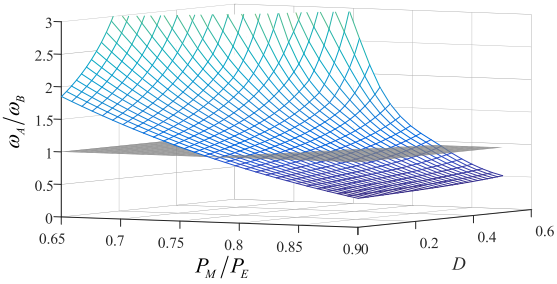

FIGURE 7. Effective boundary 3D map.

The inertia constant, M, of the generator is its inherent property, and the main reason for the system's instability of is the external unbalanced power. It can be seen from our analysis results that the correlation between ω_A/ω_B and M is insignificant, so the influence of M on ω_A/ω_B is ignored. The correlation between electromagnetic power P_E and mechanical power P_M on ω_A/ω_B is far less than that between P_M/P_E and ω_A/ω_B. Therefore, in order to simplify the subsequent analysis, P_E, P_M can be converted into P_M/P_E for analysis and calculation purposes. The correlation between D and ω_A/ω_B of system damping is obvious and should be included in the scope of subsequent analysis.

After correlation analysis, M is screened out, P_E and P_M is simplified to P_M/P_E for analysis, and the data matrix A is changed into:

$$A = \begin{bmatrix} D_1 & \frac{P_{m1}}{P_{e1}} & \omega_{A1} & \omega_{B1} \\ D_2 & \frac{P_{m2}}{P_{e2}} & \omega_{A2} & \omega_{B2} \\ \vdots & & & \\ D_n & \frac{P_{mn}}{P_{en}} & \omega_{An} & \omega_{Bn} \end{bmatrix} \tag{12}$$

Equation (10) changes to $f(D, P_M/P_E) > 1$, and $f(D, P_M/P_E) = 1$ is the critical operating conditions for phase sequence exchange.

Take P_M/P_E as the x-axis, D as the y-axis, and ω_A/ω_B as the z-axis. Use $z = 1$ plane to cut the surface as shown in Fig. 7:

The intersection of the $z = 1$ plane and the 3D surface is projected onto the x-y plane, as shown in Fig. 8:

The projection of the intersection line is $f(D, P_M/P_E) = 1$, which is the effective boundary. Let P_M/P_E be the independent variable x and D be the dependent variable y, and fit the intersection projection. The fitting results are as follows:

Where F is the significant test value, C is the constant term, b_1 is the coefficient of the first order, b_2 is the coefficient of the quadratic term. The fitting of quadratic function R^2 is closest to 1, so the result is the best [35]. The approximate analytical expression of $f(D, P_M/P_E) = 1$ is:

$$Y = 13.714X^2 - 15.01X + 3.4 \tag{13}$$

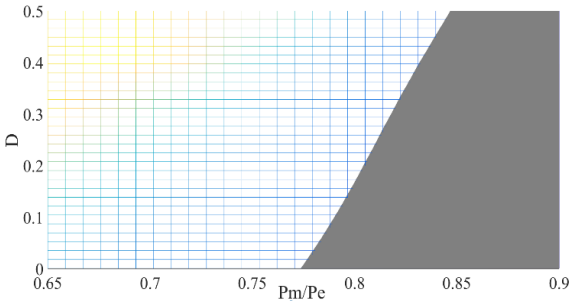

FIGURE 8. Effective boundary projection.

TABLE 3. Units for magnetic properties.

equation	R^2	F	C	b_1	b_2
Linear	0.988	5926.64	-5.482	7.067	
Quadratic	1.000	11900.61	3.400	-15.010	13.714

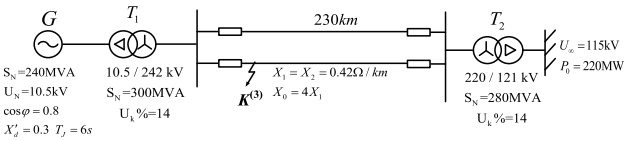

FIGURE 9. OMIB model.

Equation (13) is the effective criterion of phase sequence exchange technology, that is.

$$D > 13.714 \cdot \left(\frac{P_M}{P_E}\right)^2 - 15.01 \cdot \frac{P_M}{P_E} + 3.4 \qquad (14)$$

where $\delta_s = \arcsin\left(P_M / P_E\right)$, so effective criterion can also be.

$$\delta_s < \arcsin\left(\frac{15.01 + \sqrt{54.856 \cdot D + 38.7897}}{27.428}\right) \qquad (15)$$

where δ_s is the stable equilibrium point after fault removal, and D is the damping coefficient. After the fault is removed, the parameters of the system conform to the Equation (15), and the phase-shifting technique is shown to be effective.

IV. A TUTORIAL EXAMPLE

A. POWER SYSTEM MODEL

This section uses Simulink to build a simulation model to verify the effectiveness of the commutation sequence technique. We use the OMIB model as shown in Fig. 9.

The other parameters are set as follows: Generator damping coefficient $D = 0.8$. Generator stator resistance $r_G = 0.03pu$. Leakage resistance of transformer $r_T = 0.014pu$. Line resistance $r_l = 0.042\Omega/km$. Ground capacitance $C_l = 1.126 * 10^{-10} F/km$, where ''pu'' stands for per-unit.

B. SIMULATION ANALYSIS

When the system is steady, the double-circuit lines run parallel. The line is disconnected at $t = 1s$. The power angle curve and the output electrical power curve are shown in Figs. 10(a) and (b). The corresponding power angle curve and $\delta - \Delta\omega$ trajectory are shown in Figs. 10(c) and (d).

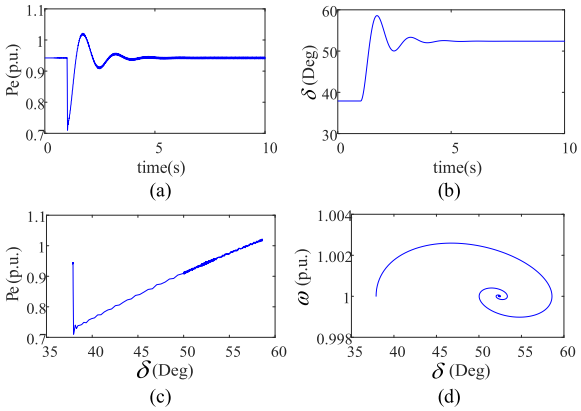

FIGURE 10. Simulations of the single circuit line. (a) Power angle curve. (b) Output electrical power curve. (c) Power-angle curve. (d) $\delta - \Delta\omega$ trajectory.

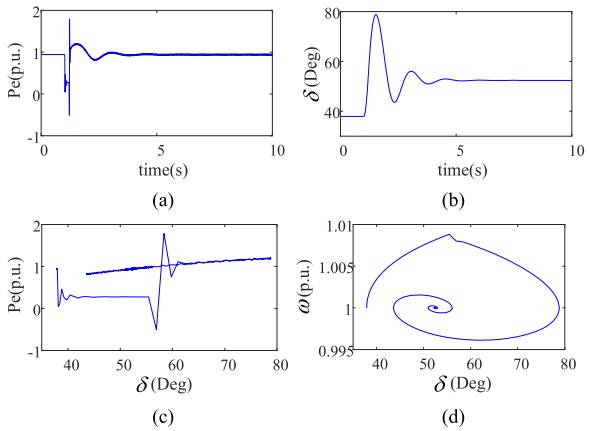

FIGURE 11. Simulations of the fault [1.2s]. (a) Power angle curve. (b) Output electrical power curve. (c) Power angle curve. (d) $\delta - \Delta\omega$ trajectory.

In a running operation with double-circuit lines, the power angle of the stable equilibrium point is $\delta_0 = 37.96°$. After disconnecting a line, the output electrical power of the system is reduced. After a period of oscillation, the system reaches a stable state at the new stable equilibrium point, and the power angle is stabilized at $\delta_s = 52.45°$.

If a three-phase short-circuit fault occurs at the beginning of a line at $t = 1s$ the fault line is cut off at $t = 1.2s$ and $t = 1.5s$. The power angle curve, the output electrical power curve, the corresponding power-angle curve and $\delta - \Delta\omega$ trajectory at the two cut-off times are shown below.

For Fig. 11, the fault line was cut off at $t = 1.2s$. After a small oscillation, the system quickly transitioned to a new stable equilibrium point and was basically stable at $t = 4s$.

For Fig. 12, the fault line was cut off at $t = 1.5s$. Due to the late removal of the fault, in Fig. 12(c), the acceleration area of the system is greater than the deceleration area, and the system experiences a loss of synchronism.

According to the third section, the system parameters meet the effective criterion of the PSET. For the case of a

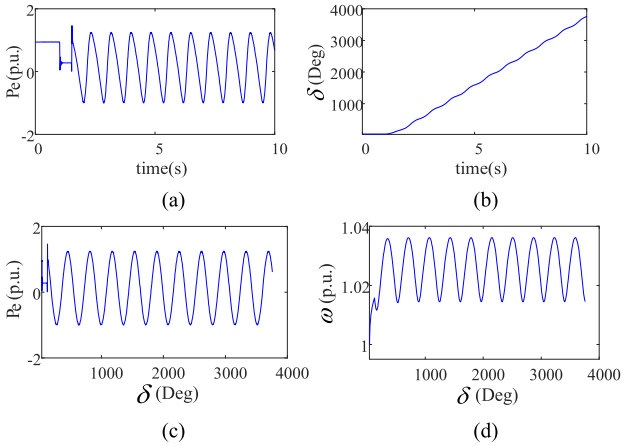

FIGURE 12. Simulations of the fault [1.5s]. (a) Power angle curve. (b) Output electrical power curve. (c) Power angle curve. (d) $\delta - \Delta\omega$ trajectory.

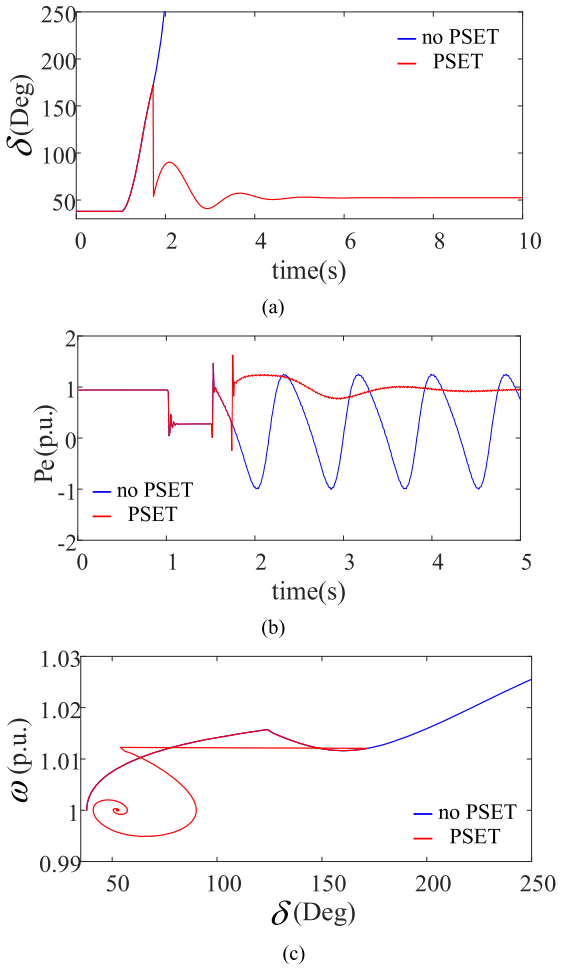

FIGURE 13. Simulations of the PSET. (a) Power angle curve. (b) Output electrical power curve. (c) $\delta - \Delta\omega$ trajectory.

1.5 second resection fault, the PSET in this paper is used to suppress the system entering an out-of-step condition. In this simulation, using the circuit breaker to realize the PSET. The stable equilibrium point after fault removal is $\delta_s = 52.45°$, therefore, the power angle threshold of PSET is set to $\delta_s + 120°$ that is $\delta_m = 172.45°$. When the system is out-of-step and the power angle swings to 172.45° the phase sequence exchange occurs. The power angle curve and the output electrical power curve after the phase sequence exchange are shown in Figs. 13(a) and (b), the corresponding $\delta - \Delta\omega$ trajectory is shown in Figs. 13 (c).

Fig. 13(a) shows the phase sequence exchange causing the work angle to instantaneously decrease by 120°, from 172.45° to 52.45°. The system then oscillates into a stable state after about 2 seconds.

Fig. 13(b) illustrates how the originally reduced electromagnetic power increases once again, expanding the deceleration area of the system and suppressing system out-of-step.

Fig. 13(c) depicts how, after the fault is removed, the power angle continuously increases. After the system enters the deceleration area the speed drops, the phase sequence exchange reduces the power angle of the system by 120°, and the system stabilizes at a new stable equilibrium point after several oscillations.

In summary, the PSET prevents the system from entering an out-of-step condition and provides new leads in the search for a solution for transient instability problem.

V. CONCLUSION

This paper proposes a new stable control measure - "phase sequence exchange technology" or PSET. PSET has the ability to restrain a system from becoming out-of-step while still maintaining the structural integrity of the power grid. This paper explains the mechanism of the phase-shifting technique that is used to improve the stability of the system, as well as determining evaluation criteria for PSET. The effective criteria for PSET is based on the system's parameters after fault resection is given. Finally, our simulation results demonstrate the effectiveness PSET.

PSET has great potential but still needs to be further explored. Future work will focus on calculating the impact of phase sequence exchanges on the system, as well as broadening the use of PSET scenarios in order to promote the application of PSET across a variety of complex systems.

REFERENCES

[1] M. T. Alam and Q. Ahsan, "A mathematical model for the transient stability analysis of a simultaneous AC–DC power transmission system," *IEEE Trans. Power Syst.*, vol. 33, no. 4, pp. 3510–3520, Jul. 2018.
[2] B. Kocuk, S. S. Dey, and X. A. Sun, "New formulation and strong MISOCP relaxations for AC optimal transmission switching problem," *IEEE Trans. Power Syst.*, vol. 32, no. 6, pp. 4161–4170, Nov. 2017.
[3] G. Gan, Z. Zhu, G. Geng, and Q. Jiang, "An efficient parallel sequential approach for transient stability emergency control of large-scale power system," *IEEE Trans. Power Syst.*, vol. 33, no. 6, pp. 5854–5864, Nov. 2018.
[4] X. Xu, H. Zhang, C. Li, Y. Liu, W. Li, and V. Terzija, "Optimization of the event-driven emergency load-shedding considering transient security and stability constraints," *IEEE Trans. Power Syst.*, vol. 32, no. 4, pp. 2581–2592, Jul. 2017.
[5] P. Bhui and N. Senroy, "Real-time prediction and control of transient stability using transient energy function," *IEEE Trans. Power Syst.*, vol. 32, no. 2, pp. 923–934, Mar. 2017.
[6] H. Fujita, H. Akagi, and Y. Watanabe, "Dynamic control and performance of a unified power flow controller for stabilizing an AC transmission system," *IEEE Trans. Power Electron.*, vol. 21, no. 4, pp. 1013–1020, Jul. 2006.

[7] J. Zuo, B. Zhang, M. Xiang, Y. Shen, and Y. Chen, "Study of transient voltage stability with transient stability probing method in hunan power grid," in *Proc. 4th Int. Conf. Syst. Inform. (ICSAI)*, Hangzhou, China, Nov. 2017, pp. 252–256.

[8] S. Das and V. K. Yadav, "Stability analysis, chaos control of fractional order Vallis and El-Nino systems and their synchronization," *IEEE/CAA J. Automatica Sinica*, vol. 4, no. 1, pp. 114–124, Jan. 2017.

[9] F. Milano and Á. O. Manjavacas, "Frequency-dependent model for transient stability analysis," *IEEE Trans. Power Syst.*, vol. 34, no. 1, pp. 806–809, Jan. 2019.

[10] Á. Ortega and F. Milano, "Stochastic transient stability analysis of transmission systems with inclusion of energy storage devices," *IEEE Trans. Power Syst.*, vol. 33, no. 1, pp. 1077–1079, Jan. 2018.

[11] Q. Jiang, Y. Wang, and G. Geng, "A parallel reduced-space interior point method with orthogonal collocation for first-swing stability constrained emergency control," *IEEE Trans. Power Syst.*, vol. 29, no. 1, pp. 84–92, Jan. 2014.

[12] L. Tang and W. Sun, "An automated transient stability constrained optimal power flow based on trajectory sensitivity analysis," *IEEE Trans. Power Syst.*, vol. 32, no. 1, pp. 590–599, Jan. 2017.

[13] M. M. Eladany, A. A. Eldesouky, and A. A. Sallam, "Power system transient stability: An algorithm for assessment and enhancement based on catastrophe theory and FACTS devices," *IEEE Access*, vol. 6, pp. 26424–26437, 2018.

[14] W. J. Huang and S. I. Liu, "Capacitor-free low dropout regulators using nested Miller compensation with active resistor and 1-bit programmable capacitor array," *IET Circuits, Devices Syst.*, vol. 2, no. 3, pp. 306–316, Jun. 2008.

[15] M. Moghbel, M. A. S. Masoum, A. Fereidouni, and S. Deilami, "Optimal sizing, siting and operation of custom power devices with STATCOM and APLC functions for real-time reactive power and network voltage quality control of smart grid," *IEEE Trans. Smart Grid*, vol. 9, no. 6, pp. 5564–5575, Nov. 2018.

[16] A. B. Birchfield, T. Xu, and T. J. Overbye, "Power flow convergence and reactive power planning in the creation of large synthetic grids," *IEEE Trans. Power Syst.*, vol. 33, no. 6, pp. 6667–6674, Nov. 2018.

[17] T. Han, Y. Chen, J. Ma, Y. Zhao, and Y.-Y. Chi, "Surrogate modeling-based multi-objective dynamic VAR planning considering short-term voltage stability and transient stability," *IEEE Trans. Power Syst.*, vol. 33, no. 1, pp. 622–633, Jan. 2018.

[18] Y. Zhang and L. Xie, "A transient stability assessment framework in power electronic-interfaced distribution systems," *IEEE Trans. Power Syst.*, vol. 31, no. 6, pp. 5106–5114, Nov. 2016.

[19] A. Pizano-Martínez, C. R. Fuerte-Esquivel, E. A. Zamora-Cárdenas, and J. M. Lozano-García, "Directional derivative-based transient stability-constrained optimal power flow," *IEEE Trans. Power Syst.*, vol. 32, no. 5, pp. 3415–3426, Sep. 2017.

[20] Z. Yao, "A control-oriented energy function for generation shedding determination for transient stability control," *IEEE Trans. Power Syst.*, vol. 34, no. 1, pp. 413–421, Jan. 2019.

[21] B. Carminati, E. Ferrari, and M. Guglielmi, "Detection of unspecified emergencies for controlled information sharing," *IEEE Trans. Dependable Secure Comput.*, vol. 13, no. 6, pp. 630–643, Nov./Dec. 2016.

[22] H. Liu, J. Su, J. Qi, N. Wang, and C. Li, "Decentralized voltage and power control of multi-machine power systems with global asymptotic stability," *IEEE Access*, vol. 7, pp. 14273–14282, 2019.

[23] S. Ghosh, K. A. Folly, and A. Patel, "Synchronized versus non-synchronized feedback for speed-based wide-area PSS: Effect of time-delay," *IEEE Trans. Smart Grid*, vol. 9, no. 5, pp. 3976–3985, Sep. 2018.

[24] Y. Wang, P. Yemula, and A. Bose, "Decentralized communication and control systems for power system operation," *IEEE Trans. Smart Grid*, vol. 6, no. 2, pp. 885–893, Mar. 2015.

[25] M. Klein, G. J. Rogers, and P. Kundur, "A fundamental study of inter-area oscillations in power systems," *IEEE Trans. Power Syst.*, vol. 6, no. 3, pp. 914–921, Aug. 1991.

[26] A. A. Hashmani and I. Erlich, "Delayed-input power system stabilizer using supplementary remote signals," *Control Eng. Pract.*, vol. 19, no. 8, pp. 893–899, Aug. 2011.

[27] H. Johal and D. Divan, "Design considerations for series-connected distributed FACTS converters," *IEEE Trans. Ind. Appl.*, vol. 43, no. 6, pp. 1609–1618, Nov. 2007.

[28] Y. Li, C. Rehtanz, S. Ruberg, L. Luo, and Y. Cao, "Wide-area robust coordination approach of HVDC and FACTS controllers for damping multiple interarea oscillations," *IEEE Trans. Power Del.*, vol. 27, no. 3, pp. 1096–1105, Jul. 2012.

[29] P. Pourbeik, P. S. Kundur, and C. W. Taylor, "The anatomy of a power grid blackout—Root causes and dynamics of recent major blackouts," *IEEE Power Energy Mag.*, vol. 4, no. 5, pp. 22–29, Sep./Oct. 2006.

[30] K. Sun, D.-Z. Zheng, and Q. Lu, "A simulation study of OBDD-based proper splitting strategies for power systems under consideration of transient stability," *IEEE Trans. Power Syst.*, vol. 20, no. 1, pp. 389–399, Feb. 2005.

[31] L. F. C. Alberto and N. G. Bretas, "Damping estimation for multi-swing transient stability analysis: The OMIB case," in *Proc. Int. Conf. Power Syst. Technol.*, vol. 2, Aug. 1998, pp. 1383–1387.

[32] Y. Xue, TH. Van Cutsem, and M. Ribbens-Pavella, "A simple direct method for fast transient stability assessment of large power systems," *IEEE Trans. Power Syst.*, vol. PWRS-3, no. 2, pp. 400–412, May 1988.

[33] H.-D. Chang, C.-C. Chu, and G. Cauley, "Direct stability analysis of electric power systems using energy functions: Theory, applications, and perspective," *Proc. IEEE*, vol. 83, no. 11, pp. 1497–1529, Nov. 1995.

[34] J. Zhou and Y. Ohsawa, "Improved swing equation and its properties in synchronous generators," *IEEE Trans. Circuits Syst. I, Reg. Papers*, vol. 56, no. 1, pp. 200–209, Jan. 2009.

[35] A. Zaidi and Q. Cheng, "An approximation solution of the swing equation using particle swarm optimization," in *Proc. IEEE Conf. Technol. Sustainability (SusTech)*, Long Beach, CA, USA, Nov. 2018, pp. 1–5.

SHAOFENG HUANG (M'08) was born in Fujian, China, in 1958. He received the bachelor's degree in electrical engineering from North China Electric Power University, Baoding, China, in 1982. He is currently a Professor with the Electrical Engineering Department, North China Electric Power University, Beijing, China. His current research interest includes power system automation and protection.

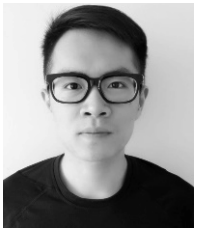

YIFAN LI was born in Shandong, China, in 1994. He received the B.S. degree in electrical engineering from North China Electric Power University (NCEPU), in 2016, where he is currently pursuing the Ph.D. degree in electrical engineering with the State Key Laboratory for Alternate Electrical Power System with Renewable Energy Sources. His current research interests include power system emergency control and transient stability.

HUI LI was born in Shandong, China, in 1994. She received the B.S. degree in electrical engineering from North China Electric Power University, Beijing, China, in 2016, where she is currently pursuing the Ph.D. degree. Her current research interest includes stability analysis of power systems.

YILING HUANG was born in Fujian, China, in 1996. He received the bachelor's degree in electrical engineering and automation from North China Electric Power University, in 2018, where he is currently pursuing the master's degree in electrical engineering. His current research interest includes power system protection.